

EQUIPARTITIONING IN LINEAR ACCELERATORS*

R. A. Jameson, AT-DO (MS 820)
 Los Alamos National Laboratory, Los Alamos, New Mexico 87545

Summary

Emittance growth has long been a concern in linear accelerators, as has the idea that some kind of energy balance, or equipartitioning, between the degrees of freedom, would ameliorate the growth.¹ M. Promé² observed that the average transverse and longitudinal velocity spreads tend to equalize as current in the channel is increased, while the sum of the energy in the system stays nearly constant. However, only recently have we shown³ that an equipartitioning requirement on a bunched injected beam can indeed produce remarkably small emittance growth. The simple set of equations leading to this condition are outlined below. At the same time, Hofmann,⁴ using powerful analytical and computational methods, has investigated collective instabilities in transported beams and has identified thresholds and regions in parameter space where instabilities occur. This is an important generalization. Work that he will present at this conference shows that the results are essentially the same in r-z coordinates for transport systems, and I will present evidence below that shows transport system boundaries to be quite accurate in computer simulations of accelerating systems also. Discussed are preliminary results of efforts to design accelerators that avoid parameter regions where emittance is affected by the instabilities identified by Hofmann. These efforts suggest that other mechanisms are present. The complicated behavior of the RFQ linac in this framework also is shown.

Conditions for Equipartitioning

A simple derivation⁵ for energy balance in a weakly coupled harmonic oscillator system requires equality of the average kinetic and potential energies in each degree of freedom; $\langle 1/2 m v_i^2 \rangle = \langle 1/2 k_i x_i^2 \rangle$, where k_i is the appropriate force constant. If we characterize the motion in terms of the oscillation's phase advance over an accelerator system period, we can write the mean-square velocity as $\langle v_i^2 \rangle = \sigma_i^2 \langle x_i^2 \rangle / N b \lambda$. At a location where the correlation $\langle x_i v_i \rangle$ is zero, rms emittance

is defined as $\epsilon_i = \langle x_i^2 \rangle^{1/2} \langle v_i^2 \rangle^{1/2}$, and the two envelope equations, useful in accelerator motion, follow directly.

$$\epsilon_t = \sigma_t^2 a^2 / N b \lambda, \quad \epsilon_l = \sigma_l^2 b^2 / N b \lambda, \quad (1)$$

in terms of longitudinal and transverse planes, where a is the average transverse rms beam radius, and $2b$ is the physical rms bunch length. The emittances are unnormalized, and we define both phase

advances over the same focusing period. It can be shown rigorously that Eq. (1) describes the matched envelope equations ($\ddot{a} = \ddot{b} = 0$), for the rms envelope behavior of particle distributions in linearized periodic systems.

If we require equal average energy in each of the coupled degrees of freedom, by equating $\langle v_i^2 \rangle = \langle v_j^2 \rangle$ and $\sigma_i^2 \langle x_i^2 \rangle / N b \lambda = \sigma_j^2 \langle x_j^2 \rangle / N b \lambda$, we find

$$\frac{\epsilon_l}{\epsilon_t} = \frac{\sigma_t}{\sigma_l} = \frac{a}{b}. \quad (2)$$

Systems satisfying Eqs. (1) and (2) simultaneously will be both matched and equipartitioned. Both are important to minimum emittance growth.

Using the notation of Mittag,⁶ we complete the design equations for drift-tube linacs with +--+ focusing.

$$\sigma_t = \cos^{-1} \left(\cos \sigma_0^t + \frac{30 I \lambda^3 (3b - a)}{W_0 a^2 b^2} \right), \quad (3)$$

and

$$\sigma_l = 2 \cos^{-1} \left(\cos \sigma_0^l + \frac{15 I \lambda^3}{W_0 a b^2} \right),$$

where N above = 2 for a drift-tube linac, σ_0^t and σ_0^l are zero-current phase advances (σ_0^l is over one cell), I is average current over one rf cycle and W_0 is rest energy.

$$\sigma_0^t = \cos^{-1} \left[1 - \left(\frac{1}{2} - \frac{\Lambda}{3} \right) \Lambda^2 \theta_0^4 - \frac{2\pi E_0 T \lambda \sin \phi_s}{W_0 B} \right], \quad (4)$$

and

$$\sigma_0^l = \cos^{-1} \left(1 + \frac{\pi E_0 T \lambda \sin \phi_s}{W_0 B} \right),$$

Λ is the quad-filling factor, E_0 the average accelerating gradient, T = transit-time factor, λ = wavelength, ϕ_s = synchronous phase angle, and

$$\theta_0^2 = \frac{B' \beta \lambda^2}{B \rho}$$

for the case at hand, with B' the quad gradient and $B \rho$ the magnetic rigidity. We define the relation between space charge and external forces

$$\mu_t = \left[1 - (\sigma_t^t / \sigma_0^t)^2 \right] \quad \text{and} \quad \mu_l = \left[1 - (\sigma_l^l / \sigma_0^l)^2 \right].$$

Similar equations for other focusing systems, and auxiliary formulas for ellipse parameters and other quantities are derived in the literature.^{6,7}

The equations may be solved in various ways, depending on what is chosen a priori. For example, if we chose $\mu_t = 0.9$, $\sigma_0^t = 49^\circ$, $\sigma_0^l = 24.7^\circ$ using

*Work supported by the US Department of Energy.

the injection point of the FMIT drift-tube deuterium linac, taking $\epsilon_t = 0.006 \text{ cm}\cdot\text{rad}$, and requiring both matching and equipartitioning, we solve for $I = 0.120 \text{ A}$ and $b = 0.842 \text{ cm}$ (or phase spread = 17.53°), requiring $\epsilon_\ell/\epsilon_t = 0.96$. As shown in Fig. 4, Ref. 3, the rms emittance growths are only about 20% over 70 cells. In contrast, in a design using a conventional buncher in which narrow phase spreads are difficult to achieve, we might start with a phase spread nearly equal to ϕ_s . Using only Eq. (1) to match the beam, we would find that the injected beam was not equipartitioned. Figure 3, Ref. 3 is such an example, where the initial transverse and longitudinal velocity spreads are quite unequal, and the equipartitioning process during acceleration caused transverse emittance growth of magnitude (~ 2) typical of that seen in operating machines run in this way. We will now relate this result to the instabilities identified by Hofmann.

Coupling Instabilities

Expressing the channel in terms of tune depression, σ/σ_0 , in each plane and the tune ratio, Hofmann derived the eigenoscillation frequencies of anisotropic KV distributed beams in transport channels, and gives stability limits for various modes for a given emittance ratio. Figure 1 is such a chart, showing thresholds for three modes at emittance ratios of four. If σ/σ_0 is below one of the thresholds, a perturbation in the particle distribution will grow. Because emittance is a projected and averaged quantity, it is very difficult to quantify the emittance growth resulting from the change in distribution, but the effective emittance does grow. In a linac, the changing parameters with acceleration result in a trajectory

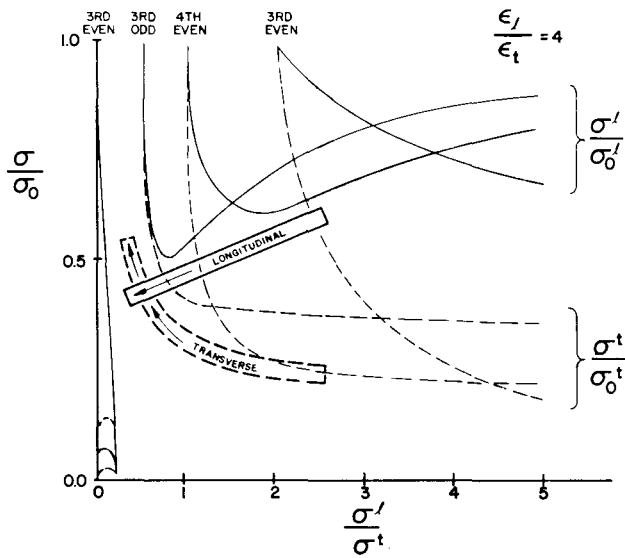


Fig. 1. Mode chart showing trajectory for initially anisotropic beam in constant $\sigma_0^t = 50^\circ$, constant E_0 linac. Moves into clear area as energies balance.

on this chart; indicated in the figure is a typical smoothed trajectory* of a linac with a large initial anisotropy between longitudinal and transverse. Because the emittance ratio is shifting, it is presently tedious to check the stability; Fig. 2 shows the unstable regions versus the rms emittance growth for a linac with a given magnetic focusing law giving constant $\sigma_0^t = 50^\circ$, constant E_0 and ϕ_s , under three conditions: (1) full nonlinear and coupled accelerating-gap transformation, (2) nonlinear gap but longitudinal-transverse

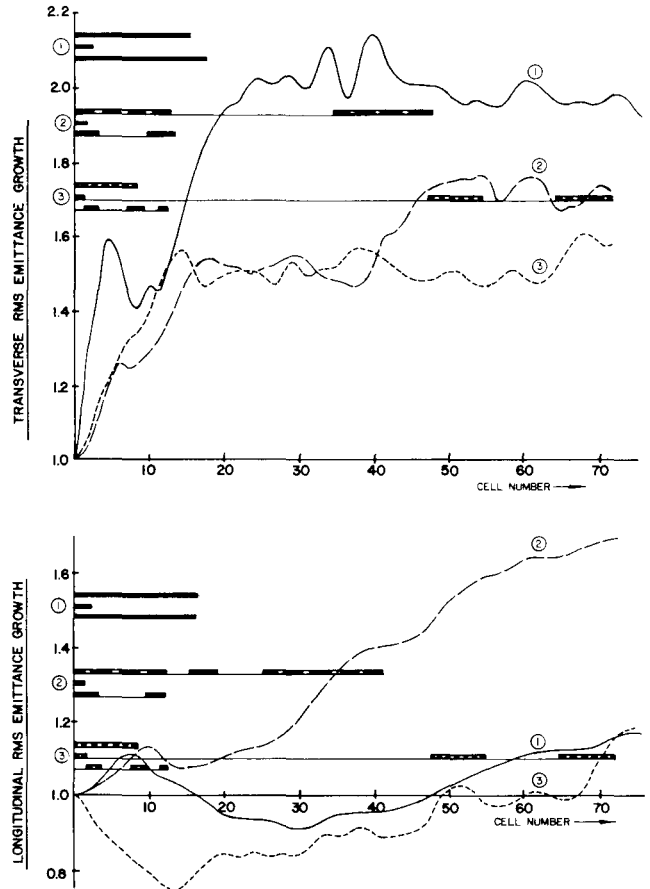


Fig. 2. Emittance growth and cells where unstable modes are excited for initially anisotropic beam in constant $\sigma_0^t = 50^\circ$, constant E_0 linac. (1) full nonlinear and coupled rf gaps. (2) nonlinear gap, longitudinal-to-transverse coupling off. (3) linearized gap, longitudinal-to-transverse coupling off. In each case, modes are top-third, odd; middle-third, even; bottom-fourth, even.

*The detailed trajectories show complicated loops as various effects oscillate and beat. The phase advances are presently computed directly from the beam properties by assuming a local match and using Eq. (1).

coupling turned off, and (3) linearized gap with λ - t coupling off. In Case 3, the effect of passing through unstable regions is quite evident as the beam initially moves toward equipartition and later receives small emittance increases. In Case 2, the third-odd mode has the major effect. The longitudinal emittance continues to grow from some other cause—probably the emittance has grown enough to be filamented by the nonlinear forces. In Case 1, the rf λ - t coupling appears to have a large effect, adding an initial peak⁸, and, after the strong initial push toward equipartition from the unstable modes, continuing in some manner to push the transverse emittance on up, while keeping the longitudinal growth smaller. By Cell 17, the trajectory on

Fig. 1 has moved into the clear zone where $\sigma^{\lambda}/\sigma^t < 0.5$ and the energies are well balanced. The longitudinal emittance has apparently remained small enough so filamentation has less effect. The growth rates when the instabilities are excited also are complicated functions; they are characterized by the plasma frequencies, which fall between the full- and zero-current frequencies. If an unstable region is entered, the energy-equalizing process drives the tunes toward a stable region, reaching it within about one plasma period in the slower of the two planes. Less free energy is then available for the next possible excursion into an unstable region to cause growth.

What would then happen if the input distribution were isotropic? This is the equipartitioned case described above; the trajectories, shown in Fig. 3, are mostly in a region free of instability. Near the end (Cells 60-72) of this system, the third-even mode is excited in the longitudinal plane, but the effect on longitudinal emittance is small because little free energy is available.

If the main eigenmode instabilities are avoided, one might expect that the simple formulas Eqs. (1) and (2) might be used to generate a linac with constant $\sigma^{\lambda}/\sigma^t$. By letting the physical beam

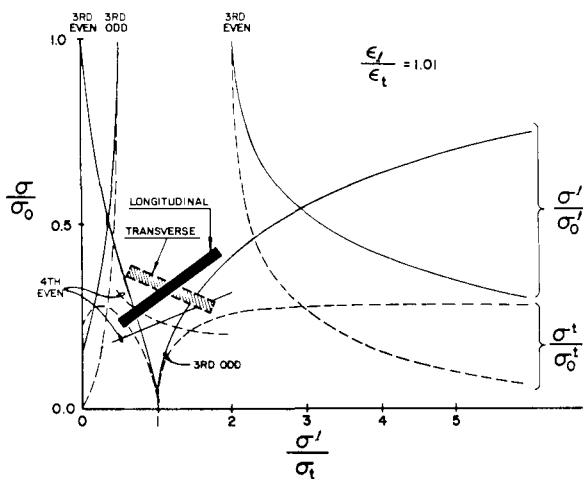


Fig. 3. Mode chart for initially equipartitioned case, constant $\mu_t = 0.9$, constant E_0 linac. Trajectories oscillate back and forth in regions shown.

length vary as $\beta^{1/3}$ to $\beta^{1/2}$, this generation was done in various ways for $\sigma^{\lambda}/\sigma^t \sim 0.9$ and $\epsilon_{\lambda}/\epsilon_t \sim 1$. However, full simulations through the resulting designs did not exhibit constant $\sigma^{\lambda}/\sigma^t$, although several gave quite low emittance growth. This is further evidence that other factors are at work.

When $\epsilon_{\lambda}/\epsilon_t \geq 4$, Hofmann's charts show a clear region where $0.25 < \sigma^{\lambda}/\sigma^t < 0.5$. Eqs. (1) and (2) were used again, with b varying as $\beta^{1/4}$, to generate three linacs, with constant emittances: $\epsilon_{\lambda}/\epsilon_t = 4$; $\sigma^{\lambda}/\sigma^t = 0.375$; and $\sigma_0^t = 90^\circ, 50^\circ$, or 40° . The depressed tunes were initialized by setting $\sigma^t/\sigma_0^t = 0.2$ and moved upward by varying E_0 , ϕ_s and the quads. This time, the prescription worked well enough that $\sigma^{\lambda}/\sigma^t$ stayed within the desired band, and $\epsilon_{\lambda}/\epsilon_t$ stayed near four. But the rms emittances did not stay constant—both grew almost linearly over the 75 cells tested. The ϵ_t growths for $\sigma_0^t = 40^\circ$ and 50° were both about a factor of 2, and x3 to 4 for $\sigma_0^t = 90^\circ$. The dif-

ference could be the influence of the 60° envelope mode. In all three cases, the ϵ_{λ} growth was about the same (x3 to 4), possibly from filamentation. Linearizing the rf gap reduced the longitudinal growth to nearly zero, without change in the transverse growth; turning off the rf coupling made little difference.

Behavior in the RFQ

The present Los Alamos RFQs use a design strategy that involves transverse matching a dc beam at injection; a shaper section, where the longitudinal rf potential well is developed and kept filled to a constant fraction of its depth; a gentle-buncher section, where the beam's physical length is kept constant, while the accelerating gradient and synchronous phase are brought to their final values; and an accelerator section, where E_0 and ϕ_s are usually held fixed. The energy increase between injection and the end of the gentle buncher is about a factor of 10, and the current-limit bottleneck occurs at the end of the gentle buncher rather than at injection. This type of RFQ design has high capture efficiency and transverse emittance growth in the area of x2 at the designated operating current, usually about half the current that could be transmitted at full saturation (with loss of about half the input current). At the operating current, we have found that the space charge to focusing force ratios μ_t and μ_{λ} are remarkably high—in the range 0.84 - 0.9. The adiabatic beam handling is clearly allowing very efficient use of the channel.

The trajectories of the Hofmann charts are intricate, with the $\epsilon_{\lambda}/\epsilon_t$ ratio passing through 1, as indicated in Fig. 4. The unstable regions are noted on the emittance-growth plot in Fig. 5; again, growth does seem to be correlated with the

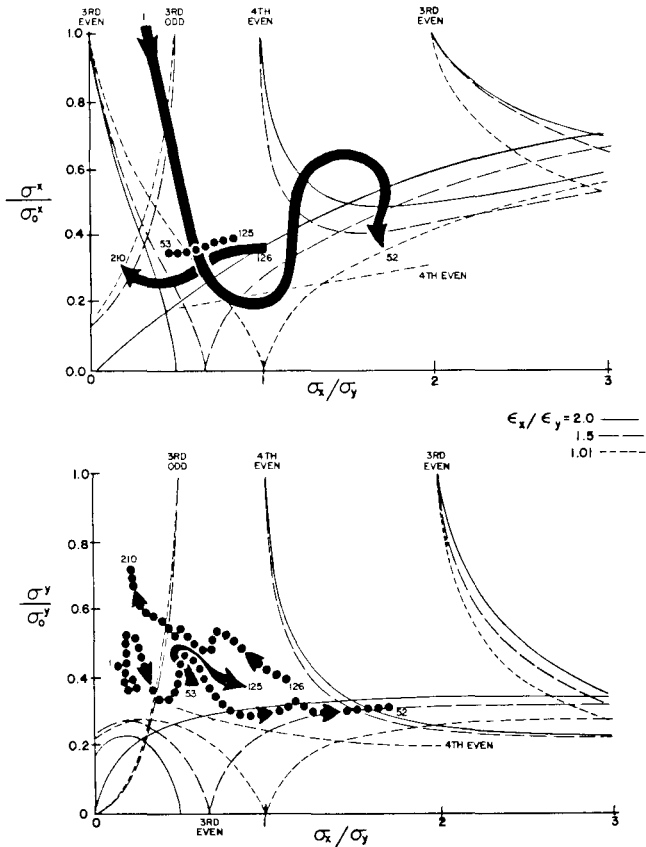


Fig. 4. RFQ mode chart. Longitudinal trajectory is solid, transverse is dotted. $\epsilon_x/\epsilon_y > 1$ until cell 52, < 1 until cell 125, then > 1 again.

collective modes and their thresholds. The velocity spreads stay equal within 25% from Cell 10 to the end in this example. Perhaps future RFQ designs can capitalize on this information.

Conclusions

The important work by Hofmann, identifying the collective modes of beam-transport systems driven by anisotropies, appears to be directly useful in accelerating channels as well. The mode charts provide a much improved cartography for estimating current limits under various conditions, and for contemplating trajectories for an accelerating system. Because equipartitioning of initial anisotropy is a self-limiting process if the unstable regions are entered, higher current limits can be expected if some of the initial emittance can be sacrificed. Initially isotropic distributions offer very good performance. The RFQ, which carefully molds a bunched distribution, can probably be made to present an optimum distribution to a following drift-tube linac. Other effects, such as external nonlinearities and couplings, still affect emittance growth in relatively less-defined ways and require further work. The behavior of total effective emittance of all the particles, important to beam losses, is still a virtually wide-open subject.

Acknowledgments

The author is indebted to R. S. Mills for computing assistance, and to I. Hofmann, R. Gluckstern, W. Lysenko, M. Reiser, and M. Pabst for many helpful discussions.

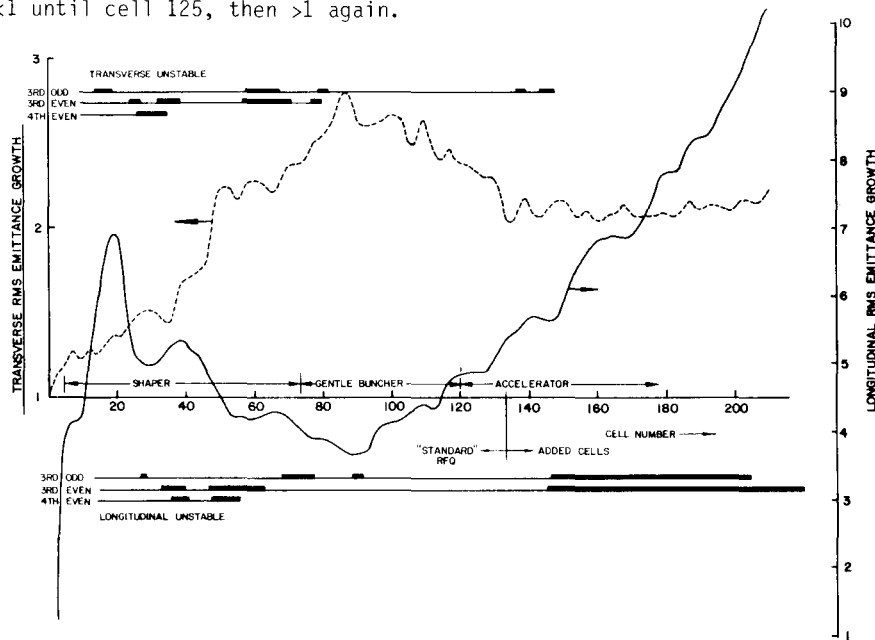


Fig. 5. Emittance growth and cells where unstable modes are excited in an RFQ. Added cells have constant E_0 & θ_s ; performance in this part should be viewed from research point of view and not necessarily as a practical design. Adding cells to RFQ avoids the matching required if transition were to drift-tube linac. The correlation of E_x growth in this section with the unstable modes is an example of better understanding of emittance growth. There is essentially no transverse rms emittance growth in the added section.

References

1. P. Lapostolle, C. Taylor, P. Tetu, and L. Thorndahl, "Intensity-Dependent Effects and Space-Charge Limit Investigations on CERN Linear Injector and Synchrotron," CERN 68 p./35 (1968).
2. M. Prome, "Effects of Space Charge in Proton Linear Accelerators," Los Alamos Scientific Laboratory translation LA-TR-79-33 from CEA-N-1457 (1971).
3. R. A. Jameson, "Beam-Intensity Limitations in Linear Accelerators," Proc. 1981 Particle Accelerator Conf., Washington, DC, March 11-13, 1981, IEEE Trans. Nucl. Sci. 28, p. 2408 (1981).
4. I. Hofmann, "Emittance Growth of Beams Close to the Space-Charge Limit," Proc. 1981 Particle Accelerator Conf., Washington, DC, March 11-13, 1981, IEEE Trans. Nucl. Sci. 28, p. 2399 (1981).
5. P. Channell, private communication.
6. K. Mittag, "On Parameter Optimization for a Linear Accelerator," Kernforschungszentrum, Karlsruhe report KFK 2555 (January 1978).
7. T. P. Wangler, "Space-Charge Limits in Linear Accelerators," Los Alamos Scientific Laboratory report LA-8388 (December 1980)
8. J. W. Staples and R. A. Jameson, "Possible Lower Limit to Linac Emittance," Proc. 1979 Particle Accelerator Conf., San Francisco, California, March 12-14, 1979, IEEE Trans. Nucl. Sci. 26, p. 3698 (1979).

Discussion

The simulation results are from full PARMILA simulations, including space charge, so the particle trajectories are as realistic as we know how to make them, and do not come from simple envelope equations. I do use the computed rms emittances and beam sizes at each cell from PARMILA in the envelope equations to get the phase advances. I tried to start with the full, very complicated rf linac, and through a series of computer experiments, to sort out some of the major effects. It is very satisfying to find that the full linac behaves in many respects nearly like the simpler transport lines that have been studied very carefully by Hofmann, Reiser, the LBL team, and others; for example, it appears that Hofmann's stability charts are also useful guides for accelerating channels.

Do the ideas we have been discussing apply to electron machines, where the acceleration is so rapid that any resonances are passed through so rapidly they would be insignificant. That is a good point; even in ion linacs there is seldom a steady-state, and this can be used to advantage for some applications. In the electron case, the ideas would apply, but I don't know how the circuit required to produce the proper fields would be made. I think there will be a growing interest in this, because there seem to be interesting requirements for high-quality, high-intensity electron beams, but most discussions start by assuming an injector.